

SWARMING OF INTERACTING ROBOTS WITH LÉVY STRATEGIES: A MACROSCOPIC DESCRIPTION.*

GISELL ESTRADA-RODRIGUEZ[†] AND HEIKO GIMPERLEIN[†]

Abstract. Lévy robotic systems combine superdiffusive random movement with emergent collective behaviour from local communication and alignment in order to find rare targets or track objects. In this article we derive macroscopic fractional PDE descriptions from the movement strategies of the individual robots. Starting from a kinetic equation which describes the movement of robots based on alignment, collisions and occasional long distance runs according to a Lévy distribution, we obtain a system of evolution equations for the fractional diffusion for long times. We show that the system allows efficient parameter studies for a target search problem, addressing basic questions like the optimal number of robots needed to cover an area in a certain time. For shorter times, in the hyperbolic limit of the kinetic equation, the PDE model is dominated by alignment, irrespective of the long range movement. This is in agreement with previous results in swarming of self-propelled particles. The article indicates the novel and quantitative modeling opportunities which swarm robotic systems provide for the study of both emergent collective behaviour and anomalous diffusion, on the respective time scales.

Key words. Anomalous diffusion, swarm robotics, velocity jump model, Lévy walk, fractional Laplacian

AMS subject classifications. 92C17, 35R11, 35Q92, 35F20

1. Introduction. The automated searching of an area for a rare target and tracking are problems of long history in different areas of computer science [8]. They include search and rescue operations in disaster regions [23], exploration for natural resources, environmental monitoring [45] and surveillance. Systems of mobile robots have inherent advantages for these applications, compared to a single robot: the parallel and spatially distributed execution of tasks gives rise to larger sensing capabilities and efficient, fault tolerant strategies. See [41] for a review in recent advances on swarm robotics and applications.

In this article we consider macroscopic PDE descriptions applicable to swarm robotic systems, which achieve scalability for a large number of independent, simple robots based on local communication and emergent collective behaviour. Much of the research focuses on determining control laws of the robot movement which give rise to a desired group behavior [6], like a prescribed spatial distribution. Typical control laws like biased random walks, reaction to chemotactic cues and long range coordination, are reminiscent of models for biological systems, and many bio-inspired strategies have been implemented in robots in recent years, for a review see [37].

Of particular recent interest have been strategies which include *nonlocal* random movements beyond Brownian motion, leading to Lévy robotics [26]. Lévy walks, with the characteristic high number of long runs, minimize the expected hitting time to reach an unknown target. These new search strategies are inspired by nonlocal movement found in a variety of organisms like T cells [20], *E. coli* bacteria [25],

*We thank Jose A. Carrillo, Siobhan Duncan, Kevin J. Painter, Jakub Stoček and Patricia A. Vargas for fruitful discussions. Jakub Stoček provided generous assistance with the numerical experiments.

Funding: G. E. R. was supported by The Maxwell Institute Graduate School in Analysis and its Applications, a Centre for Doctoral Training funded by the UK Engineering and Physical Sciences Research Council (grant EP/L016508/01), the Scottish Funding Council, Heriot-Watt University and the University of Edinburgh.

[†]Maxwell Institute for Mathematical Sciences and Department of Mathematics, Heriot-Watt University, Edinburgh, EH14 4AS, United Kingdom (ge5@hw.ac.uk, h.gimperlein@hw.ac.uk).

mussels [9] and spider monkeys [35]. Conversely, robotic systems provide controlled, quantitative models rarely available in biology.

Given sets of control laws are assessed and optimized by expensive particle based simulations and experiments with robots, based on a wide range of quality metrics [3, 6]. On the other hand, for biological systems effective macroscopic PDE descriptions have proven to be a key tool for efficient parameter optimization and analytical understanding. A series of studies dating to Patlak [33] has generated solid understanding on how microscopic detail translates into a diffusion-advection type equation [4, 47] for random walks subject to an external bias and interactions. Recent work has made progress towards nonlocal PDE descriptions of Lévy movement [15, 34, 43].

In this article, motivated by the necessity of optimal search strategies for a swarm of robots, we study a system of N individuals undergoing a velocity jump process with contact interactions and where the individuals align with their neighbors. We obtain a system of fractional PDEs for the macroscopic density $u(\mathbf{x}, t)$ and mean direction $w(\mathbf{x}, t)$:

$$(1) \quad \begin{aligned} \partial_t u + \nabla \cdot w &= 0, \\ w - \ell \frac{G(u)}{F(u)} \Lambda^w &= -\frac{1}{F(u)} C_\alpha \nabla^{\alpha-1} u, \end{aligned}$$

where Λ^w is given by (43) and $F(u)$, $G(u)$ and the diffusion constant C_α are defined in Theorem 6.1. The parameter ℓ gives the strength of the alignment. Starting from a kinetic equation that describes the movement of the individuals, combining short range interactions and alignment with occasional long runs, according to an approximate Lévy distribution, we obtain the system (1) in the appropriate parabolic time scale.

While diffusive behavior dominates for long times, swarming on shorter hyperbolic time scales is not affected by the Lévy movement, so that a rich body of work such as [5] on swarming applies to Lévy robotics. Combining long range dispersal and alignment as in the kinetic equation for the macroscopic density (31), allows us to obtain either a space fractional diffusion equation for a pure nonlocal movement of the individuals (see [15]), or a Vicsek-type equation for the case of pure alignment [10, 46].

To illustrate applications of the PDE description, Section 8 presents efficient numerical methods for the solution of (1) and applies them for some first parameter studies in the case of a search example. Detailed studies of search strategies and targeting efficiency from a robotics point of view, as well as comparisons to both standard particle simulations and experiments with *E-Puck* robots and drones are the content of forthcoming work.

Concerning previous experimental work, the particular Lévy strategy considered here, with additional long waiting times during reorientations, was implemented in a swarm robotic system of *iAnt* robots to find targets in [18], while [40] combined a Lévy walk search strategy with an added repulsion among the robots. Lévy movement directed by external cues, such as chemotaxis, has been studied in [32] to find a contaminant in water, while [30] considers sonotaxis. Efficient spatial coverage in the presence of pheromone cues was specifically addressed in [36], using an ant-inspired search strategy with long range movement.

Notation: The words *particles* and *individuals* are used interchangeably in this work. We denote the unit sphere in \mathbb{R}^n by $S = \{x \in \mathbb{R}^n : |x| = 1\}$, its surface area by $|S|$.

2. Model assumptions. A swarm robotic system [37] consists of a large number of simple independent robots with local rules, communication and interactions among them and with the environment, where the local interactions may lead to collective behaviour of the swarm. A system of *E-Puck* robots [28] in a domain in \mathbb{R}^2 provides a specific model system, to which we apply our results and present numerical experiments in Section 8. More generally, we consider N identical spherical individuals of diameter $\varrho > 0$ in \mathbb{R}^n , where $n = 2, 3$. Each individual is characterized by its position $\mathbf{x}_i \in \mathbb{R}^n$ and direction $\theta_i \in S = \{|\mathbf{x}_i| = 1\} \subseteq \mathbb{R}^n$. We assume that each individual moves according to the following rules:

1. Starting at position \mathbf{x} at time t , an individual runs in direction θ for a Lévy distributed time τ , called the “run time”.
2. The individuals move according to a velocity jump process with constant forward speed c , following a straight line motion interrupted by reorientation.
3. When the individual stops, with probability ζ it starts a long range run and tumble process, choosing a new direction θ^* according to a distribution $k(\mathbf{x}, t, \theta; \theta^*)$. With probability $(1 - \zeta)$ it aligns with the neighbors in a certain region.
4. When two individuals get close to each other they reflect elastically; the new direction is $\theta' = \theta - 2(\theta \cdot \nu)\nu$, where $\nu = \frac{\mathbf{x}_i - \mathbf{x}_j}{|\mathbf{x}_i - \mathbf{x}_j|}$ is the normal vector at the point of collision.
5. All reorientations are assumed to be instantaneous.
6. The running¹ probability ψ , which is defined as the probability that an individual moving in some fixed direction does not stop until time τ , is taken to be independent on the environment surrounding the individual.

Note that the assumptions correspond to independent individuals with simple capabilities relative to typical tasks for swarm robotic systems. They interact only with their neighbors in a fixed sensing region, and the movement decisions are based on the current positions and velocities, not information from earlier times. This assures the scalability to large numbers of robots, while nonlocal collective movement may emerge from the local rules [37].

Related movement laws have been used for target search, for example, in the experiments in [18]. Refined local control laws and the possibility for quantitative experiments with robots open up novel modeling opportunities, see Section 9.

3. Kinetic equation for microscopic movement. For the N -individual system described in Section 2, the density $\sigma = \sigma(\mathbf{x}_i, t, \theta_i, \tau_i)$ evolves according to a kinetic equation [24]

$$(2) \quad \partial_t \sigma + c \sum_{i=1}^N (\partial_{\tau_i} + \theta_i \cdot \nabla_{\mathbf{x}_i}) \sigma = - \sum_{i=1}^N \beta_i \sigma .$$

The stopping frequency β_i during a run phase relates to the probability ψ_i that an individual does not stop for a time τ_i . It is given by

$$(3) \quad \psi_i(\mathbf{x}_i, \tau_i) = \left(\frac{s_0(\rho)}{s_0(\rho) + \tau_i} \right)^\alpha, \quad \alpha \in (1, 2) .$$

This power law behaviour corresponds to the long tailed distribution of run times described in Assumption 1. in Section 2, instead of the Poisson process in classical

¹In probability this is also known as survival probability, where the “event” in this case is to stop. Hence “survival” in that context refers to the probability of continuing to move in the same direction for some time τ .

velocity jump models [31]. As the speed c of the runs is constant, the individuals perform occasional long jumps with a power-law distribution of run lengths. The stopping frequency is given by

$$(4) \quad \beta_i(\mathbf{x}_i, \tau_i) = -\frac{\partial_{\tau_i} \psi_i}{\psi_i} = \frac{\varphi_i}{\psi_i} .$$

After stopping, according to Assumption 3. individuals choose a new direction of motion by either tumbling or alignment. With probability $\zeta \in [0, 1]$ they choose a new direction according to the turning kernel T_i given by

$$(5) \quad T_i \phi(\theta_i^*) = \int_S k(\mathbf{x}_i, t, \theta_i; \theta_i^*) \phi(\theta_i) d\theta_i ,$$

where the new direction θ_i^* is symmetrically distributed with respect to the previous direction θ_i according to the distribution $k(\mathbf{x}_i, t, \theta_i; \theta_i^*) = \tilde{k}(\mathbf{x}_i, t, |\theta_i^* - \theta_i|)$ [2].

With probability $(1 - \zeta)$ the new direction of motion is aligned with the direction of the neighbors according to a distribution $\Phi(\Lambda_i \cdot \theta_i)$, with $\int_S \Phi(\Lambda_i \cdot \theta_i) d\theta_i = 1$. The average direction Λ_i at \mathbf{x}_i is defined in terms of the nonlocal flux $\mathcal{J}(\mathbf{x}_i)$ [14],

$$(6) \quad \Lambda_i(\mathbf{x}_i, t) = \frac{\mathcal{J}(\mathbf{x}_i, t)}{|\mathcal{J}(\mathbf{x}_i, t)|} , \quad \mathcal{J}(\mathbf{x}_i, t) = \int_{\mathbf{x}_j \in \mathbb{R}^n} \int_S K(|\mathbf{x}_j - \mathbf{x}_i|) p(\mathbf{x}_j, t, \theta_i) \theta_i d\mathbf{x}_j d\theta_i .$$

Here K is a given influence kernel and p is the density of individuals at \mathbf{x}_j at time t , moving in the direction θ_i .

4. Transport equation for the two-particle density. The description (2) of the N -particle problem a priori requires the understanding of collisions among the whole system of particles. In this article, however, we aim for a macroscopic description for low densities, as made precise by the scaling in Section 5. In this case collisions of more than two individuals may be neglected [7], and we truncate the hierarchy of equations by neglecting collisions of 3 or more individuals and integrate out individuals 3, ..., N from σ . The transport equation which describes the movement of two particles is given by

$$(7) \quad \partial_{\tau_1} \sigma + \partial_{\tau_2} \sigma + \partial_t \sigma + c\theta_1 \cdot \nabla_{\mathbf{x}_1} \sigma + c\theta_2 \cdot \nabla_{\mathbf{x}_2} \sigma = -(\beta_1 + \beta_2) \sigma ,$$

where $\sigma = \sigma(\mathbf{x}_1, \mathbf{x}_2, t, \theta_1, \theta_2, \tau_1, \tau_2)$ is the two-particle density function and where $\sigma(\mathbf{x}_1, \mathbf{x}_2, 0, \theta_1, \theta_2, \tau_1, \tau_2) = \sigma_0(\mathbf{x}_1^0, \mathbf{x}_2^0, 0, \theta_1^0, \theta_2^0, \tau_1^0, \tau_2^0)$. We first integrate with respect to τ_1 and τ_2 to get

$$\partial_t \tilde{\sigma} + c\theta_1 \cdot \nabla_{\mathbf{x}_1} \tilde{\sigma} + c\theta_2 \cdot \nabla_{\mathbf{x}_2} \tilde{\sigma} = -\int_0^t \beta_1 \tilde{\sigma}_{\tau_1} d\tau_1 - \int_0^t \beta_2 \tilde{\sigma}_{\tau_2} d\tau_2 + \tilde{\sigma}_{\tau_1} \Big|_{\tau_1=0} + \tilde{\sigma}_{\tau_2} \Big|_{\tau_2=0}$$

for

$$\tilde{\sigma}_{\tau_1}(\mathbf{x}_1, \mathbf{x}_2, t, \theta_1, \theta_2, \tau_1) = \int_0^t \sigma d\tau_2 , \quad \tilde{\sigma}(\mathbf{x}_1, \mathbf{x}_2, t, \theta_1, \theta_2) = \int_0^t \int_0^t \sigma d\tau_1 d\tau_2 .$$

After stopping with rate given by β_1 , from Section 3, the initial condition for the new run of individual 1 is given by

$$(8) \quad \tilde{\sigma}_{\tau_1} \Big|_{\tau_1=0}(\mathbf{x}_1, \mathbf{x}_2, t, 0, \theta_1, \theta_2) = \int_S Q(\theta_1, \theta_1^*) \int_0^t \beta_1 \tilde{\sigma}_{\tau_1}(\mathbf{x}_1, \mathbf{x}_2, t, \theta_1^*, \theta_2, \tau_1) d\tau_1 d\theta_1^* ,$$

where

$$(9) \quad Q(\theta_1, \theta_1^*) = \zeta k(\mathbf{x}_1, t, \theta_1^*; \theta_1) + (1 - \zeta) \Phi(\Lambda_1 \cdot \theta_1) .$$

In absence of collisions, for $\zeta = 0$ we recover the kinetic equation for alignment interactions as in [11, 14, 19], while for $\zeta = 1$ we obtain the long range velocity jump process from [15]. Substituting (8) and its analogue for individual 2 into the kinetic equation for $\tilde{\sigma}$, we obtain

$$(10) \quad \begin{aligned} \partial_t \tilde{\sigma} + c\theta_1 \cdot \nabla_{\mathbf{x}_1} \tilde{\sigma} + c\theta_2 \cdot \nabla_{\mathbf{x}_2} \tilde{\sigma} = & -(\mathbb{1} - \zeta T_1) \int_0^t \beta_1 \tilde{\sigma}_{\tau_1} d\tau_1 - (\mathbb{1} - \zeta T_2) \int_0^t \beta_2 \tilde{\sigma}_{\tau_2} d\tau_2 \\ & + (1 - \zeta) |S| \Phi(\Lambda_1 \cdot \theta_1) \int_0^t \beta_1 P_1 d\tau_1 + (1 - \zeta) |S| \Phi(\Lambda_2 \cdot \theta_2) \int_0^t \beta_2 P_2 d\tau_2 , \end{aligned}$$

where

$$P_1(\mathbf{x}_1, \mathbf{x}_2, t, \theta_2, \tau_1) = \frac{1}{|S|} \int_S \tilde{\sigma}_{\tau_1}(\mathbf{x}_1, \mathbf{x}_2, t, \theta_1^*, \theta_2, \tau_1) d\theta_1^*$$

and P_2 is similarly defined. Here $|S|$ denotes the surface area of the unit sphere S .

In order to write the right hand side of (10) in terms of a density independent of τ_1 and τ_2 , we introduce the density of individuals leaving \mathbf{x}_1 and \mathbf{x}_2 as

$$i_1(\mathbf{x}_1, \mathbf{x}_2, t, \theta_1, \theta_2) = \int_0^t \beta_1 \tilde{\sigma}_{\tau_1} d\tau_1 , \quad i_2(\mathbf{x}_1, \mathbf{x}_2, t, \theta_1, \theta_2) = \int_0^t \beta_2 \tilde{\sigma}_{\tau_2} d\tau_2 .$$

From the method of characteristics, we note that the solution of (7) is

$$(11) \quad \sigma = \sigma_0(\mathbf{x}_1 - c\theta_1\tau_1, \mathbf{x}_2 - c\theta_2\tau_1, t - \tau_1, \theta_1, \theta_2, 0, \tau_2 - \tau_1) \psi_1(\mathbf{x}_1, \tau_1) \psi_2(\mathbf{x}_2, \tau_2) .$$

After the scaling to macroscopic variables below, the expected run times are small and one may approximate

$$(12) \quad \sigma_0(\mathbf{x}_1, \mathbf{x}_2, t, \theta_1, \theta_2, 0, \tau_2 - \tau_1) = \sigma_0(\mathbf{x}_1, \mathbf{x}_2, t, \theta_1, \theta_2, 0, 0) + \mathcal{O}(\tau_2 - \tau_1) .$$

From (12) and (11), standard arguments as in [15] allow to write i_1 and i_2 in terms of a convolution:

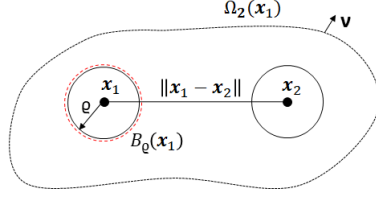
$$(13) \quad \begin{aligned} i_1(\mathbf{x}_1, \mathbf{x}_2, t, \theta_1, \theta_2) &= \int_0^t \mathcal{B}(\mathbf{x}_1, t-s) \tilde{\sigma}(\mathbf{x}_1 - c\theta_1(t-s), \mathbf{x}_2 - c\theta_2(t-s), s, \theta_1, \theta_2) ds , \\ i_2(\mathbf{x}_1, \mathbf{x}_2, t, \theta_1, \theta_2) &= \int_0^t \mathcal{B}(\mathbf{x}_2, t-s) \tilde{\sigma}(\mathbf{x}_1 - c\theta_1(t-s), \mathbf{x}_2 - c\theta_2(t-s), s, \theta_1, \theta_2) ds . \end{aligned}$$

Here the operator \mathcal{B} is defined from its Laplace transform $\hat{\mathcal{B}} = \mathcal{L}\{\mathcal{B}\}$ in time,

$$(14) \quad \hat{\mathcal{B}}(\mathbf{x}_1, \lambda + c\theta_1 \cdot \nabla_{\mathbf{x}_1} + c\theta_2 \cdot \nabla_{\mathbf{x}_2}) = \frac{\hat{\varphi}_1(\mathbf{x}_1, \lambda + c\theta_1 \cdot \nabla_{\mathbf{x}_1} + c\theta_2 \cdot \nabla_{\mathbf{x}_2})}{\hat{\psi}_1(\mathbf{x}_1, \lambda + c\theta_1 \cdot \nabla_{\mathbf{x}_1} + c\theta_2 \cdot \nabla_{\mathbf{x}_2})} ,$$

with φ_1, ψ_1 from (4). Explicit expressions for $\hat{\varphi}_1$ and $\hat{\psi}_1$ are found below in Section 6. Similarly, the terms in (10),

$$r_1(\mathbf{x}_1, \mathbf{x}_2, t, \theta_2) = \int_0^t \beta_1 P_1 d\tau_1 \quad \text{and} \quad r_2(\mathbf{x}_1, \mathbf{x}_2, t, \theta_1) = \int_0^t \beta_2 P_2 d\tau_2 ,$$

FIG. 1. *Illustration of the collision domain between two individuals.*

can be expressed in terms of \mathcal{B} . To see this, note that from (11),

$$\begin{aligned} P_1(\mathbf{x}_1, \mathbf{x}_2, t, \theta_2, \tau_1) &= \int_S \int_0^t \sigma(\mathbf{x}_1, \mathbf{x}_2, t, \theta_1, \theta_2, \tau_1, \tau_2) d\tau_2 d\theta_1 \\ (15) \qquad \qquad \qquad &= \sigma_0(\mathbf{x}_1, \mathbf{x}_2 - c\theta_2\tau_1, t - \tau_1, \theta_2, 0, 0)\psi_1, \end{aligned}$$

we obtain for the Laplace transform

$$(16) \qquad \hat{r}_1(\mathbf{x}_1, \mathbf{x}_2, \lambda, \theta_2) = \hat{\varphi}_1(\mathbf{x}_1, \lambda + c\theta_2 \cdot \nabla_{\mathbf{x}_2}) \hat{\sigma}_0(\mathbf{x}_1, \mathbf{x}_2, \lambda, \theta_2, 0, 0).$$

With

$$J_2(\mathbf{x}_1, \mathbf{x}_2, t, \theta_2) = \int_0^t P_1(\mathbf{x}_1, \mathbf{x}_2, t, \theta_2, \tau_1) d\tau_1$$

and (11), we have

$$(17) \qquad \hat{J}_2(\mathbf{x}_1, \mathbf{x}_2, \lambda, \theta_2) = \hat{\sigma}_0(\mathbf{x}_1, \mathbf{x}_2, \lambda, \theta_2, 0, 0)\psi(\mathbf{x}_1, \lambda + c\theta_2 \cdot \nabla_{\mathbf{x}_2}).$$

Combining this with (16) and (17), we obtain after an inverse Laplace transform

$$(18) \qquad r_1 = \int_0^t \mathcal{B}(\mathbf{x}_1, t-s) J_2(\mathbf{x}_1, \mathbf{x}_2 - c\theta_2(t-s), s, \theta_2) ds.$$

An analogous formula holds for r_2 . Substituting (13), (18) and its analogon for r_2 into the right hand side of (10), we obtain the following transport equation, independent of τ_1 and τ_2 ,

$$\begin{aligned} (19) \qquad \underbrace{\partial_t \tilde{\sigma}}_{(I)} &+ \underbrace{c\theta_1 \cdot \nabla_{\mathbf{x}_1} \tilde{\sigma}}_{(II)} + \underbrace{c\theta_2 \cdot \nabla_{\mathbf{x}_2} \tilde{\sigma}}_{(III)} = - \underbrace{(\mathbb{1} - \zeta T_1) i_1(\mathbf{x}_1, \mathbf{x}_2, t, \theta_1, \theta_2)}_{(IV)} \\ &- \underbrace{(\mathbb{1} - \zeta T_2) i_2(\mathbf{x}_1, \mathbf{x}_2, t, \theta_1, \theta_2)}_{(V)} + \underbrace{|S|(1 - \zeta)\Phi(\Lambda_1 \cdot \theta_1) r_1(\mathbf{x}_1, \mathbf{x}_2, t, \theta_2)}_{(VI)} \\ &+ \underbrace{|S|(1 - \zeta)\Phi(\Lambda_2 \cdot \theta_2) r_2(\mathbf{x}_1, \mathbf{x}_2, t, \theta_1)}_{(VII)}. \end{aligned}$$

From equation (19) for the two-particle density function $\tilde{\sigma}$ we now aim to derive an effective transport equation for the one-particle density function

$$(20) \qquad p(\mathbf{x}_1, t, \theta_1) = \frac{1}{|S|} \int_0^t \int_0^t \int_{\Omega_2} \int_S \sigma d\theta_2 d\mathbf{x}_2 d\tau_1 d\tau_2.$$

By integrating equation (19) with respect to the accessible phase space $(\mathbf{x}_2, \theta_2) \in \Omega_2 \times S$, where $\Omega_2 = \Omega_2(\mathbf{x}_1) = \{\mathbf{x}_2 \in \mathbb{R}^n : |\mathbf{x}_1 - \mathbf{x}_2| > \varrho\} = \mathbb{R}^n \setminus B_\varrho(\mathbf{x}_1)$ as in Figure 1, we obtain the following terms:

(I) Commuting the integrals and the time derivative results in

$$\int_{\Omega_2} \int_S \partial_t \tilde{\sigma} d\theta_2 d\mathbf{x}_2 = |S| \partial_t p .$$

(II) From Reynolds' transport theorem in the variable \mathbf{x}_2

$$c \int_{\Omega_2} \int_S \theta_1 \cdot \nabla_{\mathbf{x}_1} \tilde{\sigma} d\theta_2 d\mathbf{x}_2 = |S| c \theta_1 \cdot \nabla_{\mathbf{x}_1} p - c \int_{\partial B_e(\mathbf{x}_1)} \int_S (\theta_1 \cdot \nu) \tilde{\sigma} d\theta_2 d\mathbf{x}_2 .$$

ν is the outward pointing unit normal vector with respect to Ω_2 .

(III) From the divergence theorem

$$c \int_{\Omega_2} \int_S \theta_2 \cdot \nabla_{\mathbf{x}_2} \tilde{\sigma} d\theta_2 d\mathbf{x}_2 = c \int_{\partial B_e} \int_S (\theta_2 \cdot \nu) \tilde{\sigma} d\theta_2 d\mathbf{x}_2 ,$$

assuming that $\tilde{\sigma}$ tends to 0 sufficiently rapidly as $|x_2| \rightarrow \infty$.

(IV) Changing the order of integration we have

$$\begin{aligned} (\mathbb{1} - \zeta T_1) \int_{\Omega_2} \int_S \int_0^t \mathcal{B}(\mathbf{x}_1, t-s) \tilde{\sigma}(\mathbf{x}_1 - c\theta_1(t-s), \mathbf{x}_2 - c\theta_2(t-s), s, \theta_1, \theta_2) ds d\theta_2 d\mathbf{x}_2 \\ = |S| (\mathbb{1} - \zeta T_1) \int_0^t \mathcal{B}(\mathbf{x}_1, \theta_1, t-s) p(\mathbf{x}_1 - c\theta_1(t-s), s, \theta_1) ds . \end{aligned}$$

(V) Similar to (IV) and using

$$\int_S T\phi(\cdot, \theta) d\theta = \int_S \phi(\cdot, \eta) \int_S k(\cdot, \eta; \theta) d\theta d\eta = \int_S \phi(\cdot, \eta) d\eta = \phi(\cdot) ,$$

where ϕ is an arbitrary function, we obtain

$$\begin{aligned} \int_{\Omega_2} \int_S (\mathbb{1} - \zeta T_2) \int_0^t \mathcal{B}(\mathbf{x}_2, t-s) \tilde{\sigma}(\mathbf{x}_1 - c\theta_1(t-s), \mathbf{x}_2 - c\theta_2(t-s), s, \theta_1, \theta_2) ds d\theta_2 d\mathbf{x}_2 \\ = |S| (1 - \zeta) \int_{\Omega_2} \int_0^t \mathcal{B}(\mathbf{x}_2, t-s) J_1(\mathbf{x}_1 - c\theta_1(t-s), \mathbf{x}_2, s, \theta_1) ds d\mathbf{x}_2 . \end{aligned}$$

(VI) Moreover,

$$\begin{aligned} (1 - \zeta) \Phi(\Lambda_1 \cdot \theta_1) \int_S \int_{\Omega_2} \int_0^t \mathcal{B}(\mathbf{x}_1, t-s) J_2(\mathbf{x}_1, \mathbf{x}_2 - c\theta_2(t-s), s, \theta_2) ds d\mathbf{x}_2 d\theta_2 \\ = |S| (1 - \zeta) \Phi(\Lambda_1 \cdot \theta_1) \int_0^t \mathcal{B}(\mathbf{x}_1, t-s) u(\mathbf{x}_1, s) ds , \end{aligned}$$

where $u(\mathbf{x}_1, t)$ is a macroscopic density defined in (28).

(VII) Recalling the normalization $\int_S \Phi(\Lambda_2 \cdot \theta_2) d\theta_2 = 1$, we conclude

$$\begin{aligned} (1 - \zeta) \int_S \Phi(\Lambda_2 \cdot \theta_2) \int_{\Omega_2} \int_0^t \mathcal{B}(\mathbf{x}_2, t-s) J_1(\mathbf{x}_1 - c\theta_1(t-s), \mathbf{x}_2, s, \theta_1) ds d\mathbf{x}_2 d\theta_2 \\ = |S| (1 - \zeta) \int_{\Omega_2} \int_0^t \mathcal{B}(\mathbf{x}_2, t-s) J_1(\mathbf{x}_1 - c\theta_1(t-s), \mathbf{x}_2, s, \theta_1) ds d\mathbf{x}_2 . \end{aligned}$$

Using these, and in particular that (V) and (VII) cancel, equation (19) simplifies to

$$\begin{aligned}
\partial_t p + c\theta_1 \cdot \nabla p &= c|S|^{-1} \int_{\partial B_\varrho} \int_S \nu \cdot (\theta_1 - \theta_2) \tilde{\sigma} d\theta_2 d\mathbf{x}_2 \\
(21) \quad &+ (1 - \zeta) \Phi(\Lambda_1 \cdot \theta_1) \int_0^t \mathcal{B}(\mathbf{x}_1, t - s) u(\mathbf{x}_1, s) ds \\
&- (\mathbb{1} - \zeta T_1) \int_0^t \mathcal{B}(\mathbf{x}_1, t - s) p(\mathbf{x}_1 - c\theta_1(t - s), s, \theta_1) ds .
\end{aligned}$$

To summarize, the transport equation (21) describes the evolution of the one-particle density function $p(\mathbf{x}_1, t, \theta_1)$. The three terms on the right hand side describe the collisions, the alignment and the long range velocity jump process.

4.1. Description of one-particle density in N-particle system. For later convenience we rewrite the collision term $\int_{\partial B_\varrho} \int_S \nu \cdot (\theta_1 - \theta_2) \tilde{\sigma} d\theta_2 d\mathbf{x}_2$ as in [Appendix A](#). Summing over the $N - 1$ individuals which individual 1 can collide with, equation (21) turns into

$$\begin{aligned}
\partial_t p + c\theta_1 \cdot \nabla_{\mathbf{x}_1} p &= (1 - \zeta) \Phi(\Lambda_1 \cdot \theta_1) \int_0^t \mathcal{B}(\mathbf{x}_1, t - s) u(\mathbf{x}_1, s) ds \\
(22) \quad &- (\mathbb{1} - \zeta T_1) \int_0^t \mathcal{B}(\mathbf{x}_1, t - s) p(\mathbf{x}_1 - c\theta_1(t - s), s, \theta_1) ds \\
&+ |S|^{-1} c \varrho^{n-1} (N - 1) \int_{S_+} \int_S \nu \cdot (\theta_1 - \theta_2) \left[\tilde{\sigma}(\mathbf{x}_1, \mathbf{x}_1 - \nu \varrho, t, \theta'_1, \theta'_2) \right. \\
&\left. - \tilde{\sigma}(\mathbf{x}_1, \mathbf{x}_1 + \nu \varrho, \theta_1, \theta_2) \right] d\theta_2 d\nu .
\end{aligned}$$

From now on we work with equation (22) which describes the evolution of the one-particle density p in the system of N -particles.

5. Parabolic scaling. In applications, the mean run time $\bar{\tau}$ is often small compared with the macroscopic time scale \mathcal{T} , and we aim to study (22) for $\varepsilon = \bar{\tau}/\mathcal{T} \ll 1$ [2]. Denoting a macroscopic length scale by \mathcal{X} and $s = \frac{\mathcal{X}}{\mathcal{T}}$, we introduce normalized variables

$$t_n = \frac{t}{\mathcal{T}}, \quad \mathbf{x}_n = \frac{\mathbf{x}}{\mathcal{X}}, \quad \tau_n = \frac{\tau}{\bar{\tau}} \quad \text{and} \quad c_n = \frac{c}{s} .$$

A diffusion limit of (22) is obtained under the scaling $(\mathbf{x}, t, \tau) \mapsto (\mathbf{x}_n s/\varepsilon, t_n/\varepsilon, \tau_n/\varepsilon^\mu)$, with $c_n = \varepsilon^{-\gamma} c_0$ for $\mu, \gamma > 0$. We further assume that the diameter of each particle is small, $\varrho = \varepsilon^\xi$, while the number of particles N is large so that $(N - 1)\varrho = \varepsilon^{\xi - \vartheta}$, with $\xi - \vartheta < 0$. The scaling of the alignment is $\varepsilon^{-\eta}$.

In the normalized variables equations (4) and (3) become

$$(23) \quad \beta_\varepsilon(\mathbf{x}_1, \tau_1) = \frac{\alpha \varepsilon^\mu}{s_0 \varepsilon^\mu + \tau_1}, \quad \psi_\varepsilon(\mathbf{x}_1, \tau_1) = \left(\frac{s_0 \varepsilon^\mu}{s_0 \varepsilon^\mu + \tau_1} \right)^\alpha .$$

Here and in the following we suppress the subscript n for the new variables. Similarly,

equation (22) now reads

$$\begin{aligned}
 (24) \quad & \varepsilon \partial_t p + \varepsilon^{1-\gamma} c_0 \theta_1 \cdot \nabla p = \varepsilon^{-\eta} (1 - \zeta) \Phi^\varepsilon(\Lambda_1 \cdot \theta_1) \int_0^t \mathcal{B}^\varepsilon(\mathbf{x}_1, t-s) u(\mathbf{x}_1, s) ds \\
 & - (\mathbf{1} - \zeta T_1) \int_0^t \mathcal{B}^\varepsilon(\mathbf{x}_1, t-s) p(\mathbf{x}_1 - c\theta_1(t-s), s, \theta_1) ds \\
 & + \varepsilon^{\xi-\vartheta-\gamma} |S|^{-1} c_0 \int_{S_+} \int_S \nu \cdot (\theta_1 - \theta_2) \left[\tilde{\sigma}(\mathbf{x}_1, \mathbf{x}_1 - \varepsilon^\xi \nu, t, \theta'_1, \theta'_2) \right. \\
 & \left. - \tilde{\sigma}(\mathbf{x}_1, \mathbf{x}_1 + \varepsilon^\xi \nu, \theta_1, \theta_2) \right] d\theta_2 d\nu ,
 \end{aligned}$$

in dimension 2, where the operator in the second convolution is given by

$$(25) \quad \hat{\mathcal{B}}^\varepsilon = \hat{\mathcal{B}}^\varepsilon(\mathbf{x}_1, \varepsilon \lambda + \varepsilon^{1-\gamma} c_0 \theta_1 \cdot \nabla) = \frac{\hat{\varphi}_1^\varepsilon(\mathbf{x}_1, \varepsilon \lambda + \varepsilon^{1-\gamma} c_0 \theta_1 \cdot \nabla)}{\hat{\psi}_1^\varepsilon(\mathbf{x}_1, \varepsilon \lambda + \varepsilon^{1-\gamma} c_0 \theta_1 \cdot \nabla)} .$$

With the above scaling, we may further simplify the collision term. Using the molecular chaos assumption for the low density of particles [17], the velocity of the individuals is approximately independent of each other, and the two-particle density approximately factors into one-particle densities:

$$\tilde{\sigma}(\mathbf{x}_1, \mathbf{x}_1 \pm \varepsilon^\xi \nu, t, \theta_1, \theta_2) = p(\mathbf{x}_1, t, \theta_1) p(\mathbf{x}_1, t, \theta_2) + \mathcal{O}(\varepsilon^\xi) .$$

Then (24) becomes

$$\begin{aligned}
 (26) \quad & \varepsilon \partial_t p + \varepsilon^{1-\gamma} c_0 \theta_1 \cdot \nabla p = \varepsilon^{-\eta} (1 - \zeta) \Phi^\varepsilon(\Lambda_1 \cdot \theta_1) \int_0^t \mathcal{B}^\varepsilon(\mathbf{x}_1, t-s) u(\mathbf{x}_1, s) ds \\
 & - (\mathbf{1} - \zeta T_1) \int_0^t \mathcal{B}^\varepsilon(\mathbf{x}_1, t-s) p(\mathbf{x}_1 - c\theta_1(t-s), s, \theta_1) ds \\
 & + \varepsilon^{\xi-\vartheta-\gamma} |S|^{-1} c_0 \int_{S_+} \int_S \nu \cdot (\theta_1 - \theta_2) \left[p(\theta'_1) p(\theta'_2) - p(\theta_1) p(\theta_2) \right] d\theta_2 d\nu .
 \end{aligned}$$

6. Fractional diffusion equation. In the above parabolic scaling, this section obtains a fractional diffusion equation from (26) for the macroscopic density of individuals moving according to the model in Section 2.

Up to lower order terms, we expand $p(\mathbf{x}_1, t, \theta_1)$ in terms of its first two moments

$$(27) \quad p(\mathbf{x}_1, t, \theta_1) = |S|^{-1} (u(\mathbf{x}_1, t) + \varepsilon^\gamma n \theta_1 \cdot w(\mathbf{x}_1, t) + o(\varepsilon^\gamma)) ,$$

where

$$(28) \quad u(\mathbf{x}_1, t) = \int_S p(\mathbf{x}_1, t, \theta_1) d\theta_1 , \quad w(\mathbf{x}_1, t) = \int_S \theta_1 p(\mathbf{x}_1, t, \theta_1) d\theta_1 .$$

Substituting (27) into (26) and integrating with respect to θ_1 , we obtain the conservation law for the macroscopic density:

$$(29) \quad \varepsilon \partial_t u(\mathbf{x}_1, t) + \varepsilon n c_0 \nabla \cdot w(\mathbf{x}_1, t) = 0 .$$

To see this, note that the integral over the right hand side of (26) vanishes: for the last term in (26) this is due to the symmetry in θ_1 and θ_2 , while for the first two terms it follows from the normalization of $\Phi(\Lambda_1 \cdot \theta_1)$, resp. T_1 , as in Section 4 above.

To complement (29), it remains to express w in terms of u . To do so, we use a quasi-static approximation for the Laplace transform of (26),

$$(30) \quad \hat{\mathcal{B}}^\varepsilon(\mathbf{x}_1, \varepsilon\lambda + \varepsilon^{1-\gamma}c_0\theta_1 \cdot \nabla) \simeq \hat{\mathcal{B}}^\varepsilon(\mathbf{x}_1, \varepsilon^{1-\gamma}c_0\theta_1 \cdot \nabla),$$

since $\gamma > 0$. Transforming back we obtain

$$(31) \quad \begin{aligned} \varepsilon\partial_t p + \varepsilon^{1-\gamma}c_0\theta_1 \cdot \nabla p &= \varepsilon^{-\eta}(1-\zeta)\Phi^\varepsilon(\Lambda_1 \cdot \theta_1) \int_0^t \mathcal{B}^\varepsilon(\mathbf{x}_1, t-s)u(\mathbf{x}_1, s)ds \\ &- (\mathbb{1} - \zeta T_1)\hat{\mathcal{B}}^\varepsilon(\mathbf{x}_1, \varepsilon^{1-\gamma}c_0\theta_1 \cdot \nabla)p \\ &+ |S|^{-1}c_0\varepsilon^{\xi-\vartheta-\gamma} \int_{S_+} \int_S \nu \cdot (\theta_1 - \theta_2) \left[p(\theta'_1)p(\theta'_2) - p(\theta_1)p(\theta_2) \right] d\theta_2 d\nu. \end{aligned}$$

Equation (25) allows to obtain an explicit expression for $\hat{\mathcal{B}}^\varepsilon(\mathbf{x}_1, \varepsilon^{1-\gamma}c_0\theta_1 \cdot \nabla)$, based on the Laplace transforms of ψ_1^ε and φ_1^ε [15]:

$$\hat{\psi}_1^\varepsilon(\mathbf{x}_1, \lambda) = a^\alpha \lambda^{\alpha-1} e^{a\lambda} \Gamma(-\alpha+1, a\lambda) \quad \text{and} \quad \hat{\varphi}_1^\varepsilon(\mathbf{x}_1, \lambda) = \alpha(a\lambda)^\alpha \Gamma(-\alpha, a\lambda) e^{a\lambda}.$$

Here $a = \varsigma_0 \varepsilon^\mu$. We conclude

$$(32) \quad \hat{\mathcal{B}}^\varepsilon(\mathbf{x}_1, \lambda) = \frac{\hat{\varphi}_1^\varepsilon(\mathbf{x}_1, \lambda)}{\hat{\psi}_1^\varepsilon(\mathbf{x}_1, \lambda)} = \frac{\alpha-1}{a} - \frac{\lambda}{2-\alpha} - a^{\alpha-2} \lambda^{\alpha-1} (\alpha-1)^2 \Gamma(-\alpha+1) + \mathcal{O}(a^{\alpha-1} \lambda^\alpha).$$

Equation (32) is the key ingredient to express w in terms of u . First rewrite (31) as

$$(33) \quad \varepsilon\partial_t p + \varepsilon^{1-\gamma}c_0\theta_1 \cdot \nabla p = \varepsilon^{-\eta}M_\varepsilon + H_\varepsilon p + \varepsilon^{\xi-\vartheta-\gamma}|S|^{-1}c_0L_\varepsilon,$$

where

$$(34) \quad M_\varepsilon = (1-\zeta)\Phi^\varepsilon(\Lambda_1 \cdot \theta_1) \int_0^t \mathcal{B}^\varepsilon(\mathbf{x}_1, t-s)u(\mathbf{x}_1, s)ds,$$

$$(35) \quad H_\varepsilon = -(\mathbb{1} - \zeta T_1)\hat{\mathcal{B}}^\varepsilon(\mathbf{x}_1, \varepsilon^{1-\gamma}c_0\theta_1 \cdot \nabla) \quad \text{and}$$

$$(36) \quad L_\varepsilon = \int_{S_+} \int_S \nu \cdot (\theta_1 - \theta_2) \left[p(\theta'_1)p(\theta'_2) - p(\theta_1)p(\theta_2) \right] d\theta_2 d\nu.$$

Substituting (27) into (33), multiplying by θ_1 and integrating with respect to this variable, we see that

$$(37) \quad \begin{aligned} \varepsilon^{\gamma+1}n\partial_t w(\mathbf{x}_1, t) + \varepsilon^{1-\gamma}c_0\nabla u(\mathbf{x}_1, t) &= \varepsilon^{-\eta} \int_S \theta_1 M_\varepsilon d\theta_1 \\ &+ |S|^{-1} \int_S \theta_1 H_\varepsilon (u(\mathbf{x}_1, t) + \varepsilon^\gamma n \theta_1 \cdot w(\mathbf{x}_1, t)) d\theta_1 + |S|^{-1} \varepsilon^{\xi-\vartheta-\gamma} c_0 \int_S \theta_1 L_\varepsilon d\theta_1. \end{aligned}$$

The following subsections compute the various terms on the right hand side of (37).

6.1. Collision interactions. The third term

$$\begin{aligned} I &= \int_S \theta_1 L_\varepsilon d\theta_1 = \int_S \int_S \int_{S_+} \theta_1 p(\mathbf{x}_1, \theta'_1) p(\mathbf{x}_1, \theta'_2) \nu \cdot (\theta_1 - \theta_2) d\nu d\theta_1 d\theta_2 \\ &\quad - \int_S \int_S \int_{S_+} \theta_1 p(\mathbf{x}_1, \theta_1) p(\mathbf{x}_1, \theta_2) \nu \cdot (\theta_1 - \theta_2) d\nu d\theta_1 d\theta_2. \end{aligned}$$

may be treated similar to [17]. From the elastic reflection $\theta'_1 - \theta_1 = -2(\theta_1 \cdot \nu)\nu$ we note $\theta'_1 \cdot \nu = -\theta_1 \cdot \nu$, so that

$$(38) \quad I = \int_S \int_S \int_{S_+} (\theta'_1 - \theta_1) p(\mathbf{x}_1, \theta_1) p(\mathbf{x}_1, \theta_2) (\theta_1 - \theta_2) \cdot \nu \, d\nu \, d\theta_1 \, d\theta_2 .$$

Using the reflection law again, we see for $n = 2$

$$(39) \quad I = -\frac{4}{3} \int_S \int_S |\theta_1 - \theta_2| \theta_1 p(\mathbf{x}_1, \theta_1) p(\mathbf{x}_1, \theta_2) \, d\theta_1 \, d\theta_2 .$$

With the expansion (27) for $p(\mathbf{x}_1, t, \theta_1)$ and,

$$p(\mathbf{x}_1, t, \theta_2) = |S|^{-1} (u(\mathbf{x}_1, t) + 2\varepsilon^\gamma \theta_2 \cdot w(\mathbf{x}_1, t)) ,$$

we conclude from (39)

$$(40) \quad \begin{aligned} I &= -\frac{4}{3|S|} \int_S \int_S |\theta_1 - \theta_2| \theta_1 \left[u^2 + 2u\varepsilon^\gamma \theta_2 \cdot w + 2u\varepsilon^\gamma \theta_1 \cdot w \right] \, d\theta_1 \, d\theta_2 \\ &= -\frac{8u\varepsilon^\gamma}{3|S|} \int_S \int_S |\theta_1 - \theta_2| \theta_1 (\theta_2 \cdot w + \theta_1 \cdot w) \, d\theta_1 \, d\theta_2 + \mathcal{O}(\varepsilon^{2\gamma}) , \end{aligned}$$

since $\int_S \theta_1 \, d\theta_1 = 0$. The integral in (40) can be computed:

$$\int_S (\theta_2 \cdot w) \left[\int_S |\theta_1 - \theta_2| \theta_1 \, d\theta_1 \right] \, d\theta_2 + \int_S \theta_1 (\theta_1 \cdot w) \left[\int_S |\theta_1 - \theta_2| \, d\theta_2 \right] \, d\theta_1 = 0 + bw .$$

Here we have used $\int_S |\theta_1 - \theta_2| \, d\theta_2 = b$ and $\int_S \theta_1 (\theta_1 \cdot w) \, d\theta_1 = w$. We conclude

$$(41) \quad I = -\varepsilon^\gamma \frac{8b}{3|S|} uw .$$

A more general expression for the case $n = 3$ can be written as $I = -\varepsilon^\gamma b_n |S|^{-1} uw$. Expression (37) is thus written in terms of the first particle only, and we drop the subscript from now on.

6.2. Alignment. To evaluate the first term on the right hand side of (37), we first compute the alignment vector. From the expressions for Λ^w and \mathcal{J} in (6) and the expansion (27), we have

$$(42) \quad \mathcal{J}(\mathbf{x}_1, t) = \frac{\varepsilon^\gamma n}{|S|} \int_{\mathbf{y}} K^\varepsilon \left(\frac{|\mathbf{y} - \mathbf{x}_1|}{\varepsilon} \right) w(\mathbf{y}, t) \, d\mathbf{y} ,$$

and therefore

$$(43) \quad \Lambda^w = \frac{\int_{\mathbf{y}} K^\varepsilon \left(\frac{|\mathbf{y} - \mathbf{x}_1|}{\varepsilon} \right) w(\mathbf{y}, t) \, d\mathbf{y}}{\left| \int_{\mathbf{y}} K^\varepsilon \left(\frac{|\mathbf{y} - \mathbf{x}_1|}{\varepsilon} \right) w(\mathbf{y}, t) \, d\mathbf{y} \right|} .$$

Now the Laplace transform of M_ε from (34) is given by

$$\hat{M}_\varepsilon = (1 - \zeta) \Phi^\varepsilon(\Lambda^w \cdot \theta) \hat{\mathcal{B}}^\varepsilon(\mathbf{x}, \varepsilon\lambda) \hat{u}(\mathbf{x}, \lambda) = (1 - \zeta) \Phi^\varepsilon(\Lambda^w \cdot \theta) \frac{\hat{\varphi}^\varepsilon(\mathbf{x}, \varepsilon\lambda)}{\hat{\psi}^\varepsilon(\mathbf{x}, \varepsilon\lambda)} \hat{u}(\mathbf{x}, \lambda) .$$

To leading order in ε we therefore deduce from the expansion (32) that

$$M_\varepsilon \simeq (1 - \zeta) \Phi^\varepsilon(\Lambda^w \cdot \theta) \frac{\varepsilon^{-\mu}(\alpha - 1)}{\varsigma_0} u(\mathbf{x}, t) .$$

Integrating over the sphere, $\Psi^\varepsilon(\Lambda^w) = \int_S \theta \Phi^\varepsilon(\Lambda^w \cdot \theta) d\theta = z \Lambda^w$, where z is given by

$$(44) \quad z = \int_0^{2\pi} \Phi^\varepsilon(\cos \theta) \cos \theta d\theta ,$$

we conclude

$$\varepsilon^{-\eta} \int_S \theta_1 M_\varepsilon d\theta_1 = \varepsilon^{-\mu-\eta} (1 - \zeta) \frac{z(\alpha - 1)}{\varsigma_0} u \Lambda^w .$$

6.3. Long range movement. The second term on the right hand side of (37) has been computed in [15]:

$$\begin{aligned} & \frac{\varepsilon^{\frac{\gamma}{\alpha-1}-1}}{|S|} \int_S \theta H_\varepsilon(u + \varepsilon^\gamma n \theta \cdot w) d\theta \simeq \\ & - \frac{\varsigma_0^{\alpha-2}}{|S|} (1 - \alpha)^2 \Gamma(-\alpha + 1) c_0^{\alpha-1} \nabla^{\alpha-1} u \left(\frac{\zeta n^2 \nu_1}{|S|} - 1 \right) + \frac{\alpha - 1}{\varsigma_0 |S|} n w (\zeta \nu_1 - 1) . \end{aligned}$$

Here ν_1 is the second eigenvalue of the operator T [2]. Substituting the results of Subsections 6.1 and 6.2 into (37) results in

$$(45) \quad \begin{aligned} \varepsilon^{\gamma+1} n \partial_t w + \varepsilon^{\gamma-1} c_0 \nabla u &= \varepsilon^{-\mu-\eta} (1 - \zeta) \frac{z(\alpha - 1)}{\varsigma_0} u \Lambda^w \\ &+ \frac{1}{|S|} \int_S \theta H_\varepsilon(u + \varepsilon^\gamma n \theta \cdot w) d\theta - \varepsilon^{\xi-\vartheta} \frac{4bc_0}{3|S|^2} n u w . \end{aligned}$$

Furthermore, using Subsection 6.3 the term of order $\varepsilon^{1-\frac{\gamma}{\alpha-1}}$ is given by

$$(46) \quad \begin{aligned} 0 &= - \frac{\varsigma_0^{\alpha-2}}{|S|} (1 - \alpha)^2 \Gamma(-\alpha + 1) c_0^{\alpha-1} \nabla^{\alpha-1} u \left(\frac{\zeta n^2 \nu_1}{|S|} - 1 \right) + \frac{\alpha - 1}{\varsigma_0 |S|} n w (\zeta \nu_1 - 1) \\ &- \frac{4bc_0}{3|S|^2} n u w + (1 - \zeta) \frac{z(\alpha - 1)}{\varsigma_0} u \Lambda^w \end{aligned}$$

provided the following scaling relations are satisfied:

$$(47) \quad \mu = \frac{1 - \alpha(1 - \gamma)}{\alpha - 1}, \quad \eta = -\gamma, \quad \text{and} \quad \xi - \vartheta = 1 - \frac{\gamma}{\alpha - 1} < 0 .$$

Here $\gamma > (\alpha - 1)/\alpha$ to guarantee that $\mu > 0$ and $\xi - \vartheta < 0$. This is in agreement with the assumption that $1 - \gamma < 1$ used in Section 6 for the quasi-static approximation in (30). As was assumed in Section 5, $\xi - \vartheta < 0$ which implies that $(N - 1)\varrho \rightarrow \infty$ as $\varepsilon \rightarrow 0$.

From (46) we obtain an expression for w and conclude the following theorem.

THEOREM 6.1. *As $\varepsilon \rightarrow 0$, the first two moments of the solution to (33) satisfy the following fractional diffusion equation for the macroscopic density $u(\mathbf{x}, t)$ and the mean direction $w(\mathbf{x}, t)$:*

$$(48) \quad \partial_t u + \nabla \cdot w = 0 ,$$

$$(49) \quad w - \ell \frac{G(u)}{F(u)} \Lambda^w = - \frac{1}{F(u)} C_\alpha \nabla^{\alpha-1} u ,$$

where Λ^w is given by (43),

$$F(u) = \frac{\alpha - 1}{\varsigma_0 |S|} n(1 - \zeta \nu_1) + \frac{8bc_0}{3|S|^2} u, \quad G(u) = (1 - \zeta) \frac{z(\alpha - 1)}{\varsigma_0} u$$

and

$$C_\alpha = -\frac{\varsigma_0^{\alpha-2} c_0^{\alpha-1} (\alpha - 1)^2 \pi (|S| - 4\zeta \nu_1)}{\sin(\pi\alpha) \Gamma(\alpha) |S|^2}.$$

Recall that the parameter ℓ in (49) describes the strength of the alignment.

Without alignment, $\zeta = 1$, the term $G(u)$ vanishes and we recover the result in [15] in the absence of chemotaxis. Appendix B discusses two different types of alignment kernels and their effect on the dynamics of the system (48)-(49).

7. Macroscopic transport equation for swarming. This section studies the PDE description of the robot movement on shorter, hyperbolic time scales, where the formation of patterns like swarming can be expected. We compare the resulting description obtained here with some classical results in [12, 29].

The hyperbolic scaling limit obtained by setting $\gamma = 0$ in Section 5, so that $\mathbf{x}_n = \varepsilon \mathbf{x}/s$, $t_n = \varepsilon t$, $\tau_n = \tau \varepsilon^\mu$. The space and time variables are on the same scale, and the quasi-static approximation in (30) is no longer justified. The kinetic equation (22) for the microscopic particle movement is therefore given by

$$\begin{aligned} \varepsilon(\partial_t p + c_0 \theta \cdot \nabla p) &= (1 - \zeta) \Phi^\varepsilon(\Lambda \cdot \theta) \int_0^t \mathcal{B}^\varepsilon(\mathbf{x}, t-s) u(\mathbf{x}, s) ds \\ &\quad - (\mathbb{1} - \zeta T) \int_0^t \mathcal{B}^\varepsilon(\mathbf{x}, t-s) p(\mathbf{x} - c\theta(t-s), s, \theta) ds. \end{aligned} \quad (50)$$

For simplicity we neglect the collision interactions. The Laplace transform of (50) is

$$\begin{aligned} \varepsilon(\lambda + c_0 \theta \cdot \nabla) \hat{p} - \varepsilon p_0 &= (1 - \zeta) \Phi^\varepsilon(\Lambda \cdot \theta) \hat{\mathcal{B}}^\varepsilon(\mathbf{x}, \varepsilon \lambda) \hat{u}(\mathbf{x}, \lambda) \\ &\quad - (\mathbb{1} - \zeta T) \hat{\mathcal{B}}^\varepsilon(\mathbf{x}, \varepsilon \lambda + \varepsilon c_0 \theta \cdot \nabla) \hat{p}, \end{aligned} \quad (51)$$

where from (32) the operator $\hat{\mathcal{B}}^\varepsilon$ takes the form

$$\hat{\mathcal{B}}^\varepsilon(\mathbf{x}, \varepsilon \lambda) = \varepsilon^{-\mu} A + \varepsilon^{\mu(\alpha-2) + \alpha - 1} B \lambda^{\alpha-1} + \mathcal{O}(\varepsilon), \quad (52)$$

with

$$A = \frac{\alpha - 1}{\varsigma_0} \quad \text{and} \quad B = -\varsigma_0^{\alpha-2} (\alpha - 1)^2 \Gamma(-\alpha + 1). \quad (53)$$

In order to obtain a conservation equation for the macroscopic density, we start from the generalized Chapman-Enskog expansion for \hat{p} in Appendix C,

$$\hat{p}(\mathbf{x}, t, \theta) = \Phi_\zeta(\theta) \hat{u} + \varepsilon^{(\mu+1)(\alpha-1)} \hat{p}_1 + \mathcal{O}(\varepsilon^{2(\mu+1)(\alpha-1)}), \quad (54)$$

with \hat{p}_1 given by (74) and $\Phi_\zeta(\theta) = (1 - \zeta) \Phi^\varepsilon(\Lambda \cdot \theta) + \zeta$. Substituting (54) into (50) and integrating over S , we obtain the conservation equation

$$\partial_t u + z c_0 (1 - \zeta) \nabla \cdot (u \Lambda) = 0. \quad (55)$$

Note that the right hand side is zero by conservation of particles, as in (29).

It remains to determine the mean direction $u\Lambda$, and for simplicity we start from (51). Substituting the expansion (54) into (51), using the definitions of \hat{p}_0 and \hat{p}_1 given in (73) and (74) respectively, and expanding in powers of ε , we find

$$(56) \quad (\lambda\Phi_\zeta\hat{u} + c_0\theta \cdot \nabla(\Phi_\zeta\hat{u})) - p_0 + \varepsilon^{(\mu+1)(\alpha-1)}(\lambda\hat{p}_1 + c_0\theta \cdot \nabla\hat{p}_1) = \mathcal{O}(\varepsilon^{(\mu+1)(2\alpha-3)}) .$$

We multiply (56) by $\theta \cdot v$, where $v \in \mathbb{R}^n$ is orthogonal to Λ , and integrate over S ,

$$(57) \quad \left[\int_S \theta(\lambda\Phi_\zeta\hat{u} + c_0\theta \cdot \nabla(\Phi_\zeta\hat{u}))d\theta - \int_S \theta p_0 d\theta \right] \cdot v + \varepsilon^{(\mu+1)(\alpha-1)} \left[\int_S \theta(\lambda\hat{p}_1 + c_0\theta \cdot \nabla\hat{p}_1) d\theta \right] \cdot v = \mathcal{O}(\varepsilon^{(\mu+1)(2\alpha-3)}) .$$

After an inverse Laplace transform and letting $\varepsilon \rightarrow 0$ we obtain, provided $\alpha > 3/2$,

$$\left(z(1-\zeta)\partial_t(u\Lambda) + c_0 \int_S \theta \cdot \nabla(u\Phi_\zeta(\theta))\theta d\theta \right) \cdot v = 0 .$$

As $v \perp \Lambda$ was arbitrary, we can reformulate this in terms of the orthogonal projection P_\perp onto Λ^\perp :

$$(58) \quad P_\perp \left(z(1-\zeta)\partial_t(u\Lambda) + c_0 \nabla \cdot u \int_S (\theta \otimes \theta)\Phi_\zeta(\theta)d\theta \right) = 0 .$$

We consider the two terms separately. Expanding the first term we have

$$(59) \quad z(1-\zeta)P_\perp(u\partial_t\Lambda + \Lambda\partial_t u) = z(1-\zeta)u\partial_t\Lambda ,$$

since $\langle \partial_t\Lambda, \Lambda \rangle = \frac{1}{2}\partial_t|\Lambda|^2 = 0$, i.e., $\Lambda \perp \partial_t\Lambda$. For the second term we compute

$$\int_S (\theta \otimes \theta)\Phi_\zeta(\theta)d\theta$$

in polar coordinates $\theta = \cos(s)\Lambda + \sin(s)\Lambda^\perp$. When $n = 2$ we find

$$(60) \quad \begin{aligned} \int_S (\theta \otimes \theta)\Phi_\zeta(\theta)d\theta &= (1-\zeta) \int_S (\theta \otimes \theta)\Phi^\varepsilon(\Lambda \cdot \theta)d\theta + \zeta \int_S (\theta \otimes \theta)d\theta \\ &= (1-\zeta) \int_0^{2\pi} \Phi^\varepsilon(\cos(s)) \begin{bmatrix} \cos^2(s) & 0 \\ 0 & \sin^2(s) \end{bmatrix} ds + \zeta \int_0^{2\pi} \begin{bmatrix} \cos^2(s) & 0 \\ 0 & \sin^2(s) \end{bmatrix} ds \\ &= (1-\zeta)(a_3\Lambda \otimes \Lambda + a_1\mathbb{1}) + \mathbb{1}\pi\zeta , \end{aligned}$$

where we have used $\Lambda^\perp \otimes \Lambda^\perp = \mathbb{1} - \Lambda \otimes \Lambda$ and $a_3 = a_0 - a_1$,

$$a_0 = \int_0^{2\pi} \Phi^\varepsilon(\cos(s)) \cos^2(s) ds , \quad a_1 = \int_0^{2\pi} \Phi^\varepsilon(\cos(s)) \sin^2(s) ds .$$

A similar result to (60) also holds for $n = 3$.

Using (60) we compute the second integral in (58) as follows

$$(61) \quad \begin{aligned} c_0 P_\perp \nabla \cdot u \int_S (\theta \otimes \theta)\Phi_\zeta(\theta)d\theta &= C_1 P_\perp \nabla \cdot (u\Lambda \otimes \Lambda) + C_2 P_\perp \nabla u \\ &= C_1 P_\perp (\Lambda \otimes \Lambda \nabla u + u\Lambda \cdot \nabla \Lambda + u(\nabla \cdot \Lambda)\Lambda) + C_2 P_\perp \nabla u \end{aligned}$$

where $C_1 = c_0(1-\zeta)a_3$ and $C_2 = c_0(1-\zeta)\mathbb{1}a_1 + c_0\mathbb{1}\pi\zeta$. Because $|\Lambda| = 1$, $\langle \Lambda \cdot \nabla \Lambda, \Lambda \rangle = \Lambda \cdot \nabla |\Lambda|^2 = 0$. Then, by definition of P_\perp we have that $P_\perp(\Lambda \cdot \nabla \Lambda) = \Lambda \cdot \nabla \Lambda$ and $P_\perp(\Lambda) = 0$, so that

$$(62) \quad c_0 P_\perp \nabla \cdot u \int_S (\theta \otimes \theta) \Phi_\zeta(\theta) d\theta = C_1 u \Lambda \cdot \nabla \Lambda + C_2 P_\perp \nabla u .$$

Substituting (59) and (62) into (58) we conclude

$$u(z(1-\zeta)\partial_t \Lambda + C_1 \Lambda \cdot \nabla \Lambda) + C_2 P_\perp \nabla u = 0 .$$

We summarize the conclusion in the following theorem.

THEOREM 7.1. *As $\varepsilon \rightarrow 0$, the solution p to the kinetic equation (50) admits an expansion*

$$p(\mathbf{x}, t, \theta) = \Phi_\zeta(\theta) u(\mathbf{x}, t) + \varepsilon^{(\mu+1)(\alpha-1)} p_1 + \mathcal{O}(\varepsilon^{2(\mu+1)(\alpha-1)})$$

with $\Phi_\zeta(\theta) = (1-\zeta)\Phi^\varepsilon(\Lambda \cdot \theta) + \zeta$. The functions u and Λ satisfy the following system of equations

$$(63) \quad \partial_t u + z c_0 (1-\zeta) \nabla \cdot (u \Lambda) = 0 ,$$

$$(64) \quad u(C_0 \partial_t \Lambda + C_1 \Lambda \cdot \nabla \Lambda) + C_2 P_\perp \nabla u = 0 .$$

Here $P_\perp = \mathbb{1} - \Lambda \otimes \Lambda$ and

$$C_0 = z(1-\zeta), \quad C_1 = c_0(1-\zeta)a_3, \quad C_2 = c_0(1-\zeta)\mathbb{1}a_1 + c_0\mathbb{1}\pi\zeta .$$

Theorem 7.1 is similar to the result of [14] for $\zeta = 0$. Note that in the hyperbolic scaling the alignment interaction dominates over the long range dispersal, so (63) and (64) are independent of the parameter α . Standard techniques for swarming and flocking thereby apply to the stochastic movement laws relevant to swarm robotic systems. For a pure long range velocity jump process, $\zeta = 1$, we get from (63) that u is constant on hyperbolic time scales. This agrees with the hyperbolic scaling for the case of the classical heat equation.

8. Lévy strategies for area coverage in robots. In this section we illustrate how **Theorem 6.1** can be used to address relevant robotics questions discussed in **Section 1**. In particular, we consider how quickly a swarm of *E-Puck* robots [28] covers a convex arena Ω . The most efficient way to search the area is deterministic, by zigzagging from one boundary of the domain to the opposite. However, this strategy proves not to be robust for practical robots which experience technical failures and does not easily scale for large numbers of robots in unknown domains. Swarm robotic systems are commonly used as an efficient and robust solution. Here we shed light on how many robots are necessary to cover a certain area in a given time, and we confirm the advantage of strategies based on Lévy walks rather than Brownian motion.

A second quantity of interest is the mean first passage time for an unknown target. In this case [16, 20] have shown analogous advantages for Lévy strategies in a system similar to **Theorem 6.1**, with delays between reorientations, but no alignment.

8.1. Area coverage for a swarm robotic system. For simplicity of the numerics we here neglect the alignment and collision terms, so that the model equations

are

$$(65) \quad \begin{aligned} \partial_t u + \nabla \cdot (C_\alpha \nabla^{\alpha-1} u) &= 0 && \text{in } \Omega \times [0, T] \\ u &= 0 && \text{in } \Omega^c \times [0, T] \\ u(\mathbf{x}, 0) &= u_0 && \text{in } \Omega. \end{aligned}$$

The numerical approximation of (65) by finite elements is described in [1, 16].

From the solution of (65) we compute the area covered as a function of time, depending on the number of robots and the parameter α .

The standard model system for *E-Puck* robots in the Robotics Lab at Heriot-Watt University consists of a rectangular arena Ω of dimensions 200 cm \times 160 cm. The diameter of each *E-Puck* robot is $\varrho = 7.5$ cm, and it moves with a speed $c = 3$ cm/s. As the scale s is of order cm/s, from the dimensions of Ω we obtain a value of $\varepsilon = 0.005$ from $\mathbf{x}_n = \varepsilon \mathbf{x}/s$. We further determine ϑ , ξ and γ from $N - 1 = \varepsilon^{-\vartheta} \gg 1$, $\varrho = \varepsilon^\xi \ll 1$ and (47) in Subsection 6.2, respectively. Finally, from $c_n = \varepsilon^{-\gamma} c_0$, we obtain the speed c_0 . More concretely, we write the remaining parameters in terms of the number of robots N and $\alpha \in (1, 2)$: $\xi = -0.38$, $c_n = 3$,

$$\vartheta = \log_{0.005}(N - 1)^{-1}, \quad \gamma = (\alpha - 1) (1.38 + \log_{0.005}(N - 1)^{-1}), \quad c_0 = 3 \cdot 0.005^\gamma.$$

These values of the parameters are in agreement with the assumptions in Section 6.

Initially the robots are placed in the center of the arena with a distribution given by $u_0(\mathbf{x}, 0) = \max\{1.2e^{-\frac{|\mathbf{x}|^2}{e^N}} - 0.2, 0\}$. The coverage at time t is defined as the area of $\{x : \int_0^t u(x, s) ds > \delta\}$, divided by the area of Ω . It depends on a threshold parameter δ , and we choose $\delta = 0.5$.

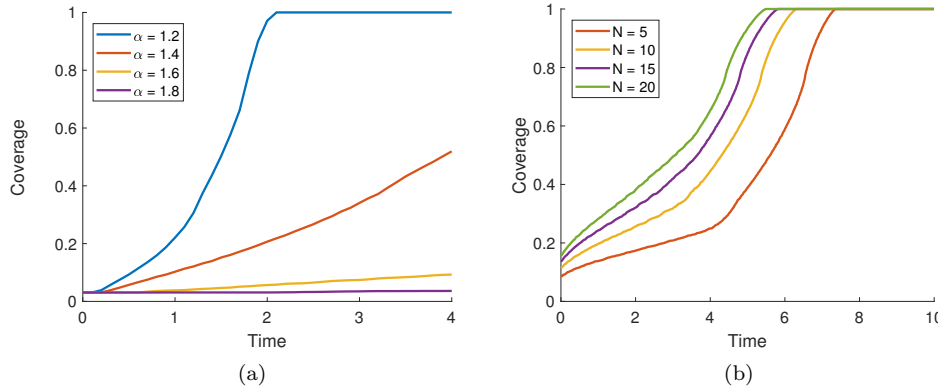


FIG. 2. Coverage as a function of time for (a) $N = 5$, varying α , (b) varying N , $\alpha = 1.2$.

Figures 2a and 2b show the coverage as a function of time as the Lévy exponent α , resp. the number N of robots, are varied. In Figure 2a, for $N = 5$ robots, the whole area is covered within approximately 2 minutes for $\alpha = 1.2$, much faster than for values of α which are closer to normal diffusion ($\alpha = 2$). This evidences improvements by long distance runs, compared with classical Brownian motion, similar to what is known for target search strategies [16, 20].

For fixed $\alpha = 1.2$, Figure 2b shows how many robots are needed to cover a given percentage of the area within time T . If the goal is to search 50% of the area in 4

minutes, 10 robots are needed to achieve the task. Clearly, the coverage does not increase linearly with the number of robots. For larger N the effect of collisions should be included, as they limit the effect of additional robots in the search. This will be part of a detailed quantitative comparison to experiments in ongoing work with computer scientists.

9. Discussion. In this paper we find macroscopic nonlocal PDE descriptions for systems arising in swarm robotics [18]. Similar to biological systems of cells or bacteria, on the microscopic scale independent agents follow a velocity jump process, for robots with collision and alignment interactions between neighbors and long range dispersal. Macroscopic swarming behaviour emerges on a hyperbolic time scale. We indicate the relevance to typical problems in swarm robotics, like target search, tracking or surveillance. Conversely, the available control in robotic systems and possibility of accurate measurements provide new modeling opportunities from microscopic to macroscopic scales.

Refined local control laws, which give rise to a desired distribution of robots, are a main topic of current research in particle swarm optimization. Biologically motivated strategies include the directed movement driven by a chemical cue, chemotaxis, which is used to devise efficient search strategies for Lévy robotic systems with sensing capabilities [36]. In bacterial foraging algorithms the length of the run or the tumbling may depend on external cues, such as pheromones, similarly leading to chemotactic behavior [44]. Also more general classes of biased random walks are of interest [13], as are control strategies obtained from machine learning. In an ongoing work we implement relevant target search strategies for systems of *E-Puck* robots and drones, which combine Lévy walks and collision avoidance with chemotaxis. The macroscopic PDE descriptions inform the optimal parameter settings in local control laws.

Similarly for the alignment, a wide range of interactions is being explored in robotic systems, see [39] and references therein. For example, in [27] the region of interaction may depend adaptively on the current distribution, with the aim of forming several clusters of robots. Follower-leader alignment strategies were combined with swarming models in [22, 38]. In [22] a “transient” leadership model was considered, imitating bird flocks, where agents react in correspondence with their neighbors, while hierarchical leadership was studied in [38] within a Cucker-Smale model.

In the tumbling process, the current paper neglects delays during reorientations; we consider the tumbling phase to be much shorter than the run phase. For the system of *iAnt* Lévy robots in [18] waiting times are relevant, and the corresponding effect can be included into the analysis as previously done in [16]: long tailed waiting times lead to additional memory effects in time, and on long (parabolic) time scales are described by space-time fractional evolution equations. Short delays in the tumbling phase affect the diffusion coefficient C_α [42].

In all cases, rapid convergence from the initial to the desired final distribution of the robotic swarm is a main goal, and recent research has started to investigate metrics which quantify the convergence [3, 6]. Our work replaces the computationally expensive particle based models used in simulations by more efficient PDE descriptions and thereby allows efficient exploration and optimization of microscopic control laws. Detailed numerical experiments which include alignment and collision avoidance, as well as their validation against concrete robotics experiments with *E-Puck* robots and drones, are pursued in a current collaboration with computer scientists. Complementary ongoing work considers Lévy movement in complex geometries, modeled by

networks of convex domains.

Appendix A. Collision term. We consider the interaction term only,

$$(66) \quad \int_{\partial B_\varrho} \int_S \nu \cdot (\theta_1 - \theta_2) \tilde{\sigma}(\mathbf{x}_1, \mathbf{x}_2, t, \theta_1, \theta_2) d\theta_2 d\mathbf{x}_2 .$$

The normal vector ν at the time of collision is given by $\nu = (\mathbf{x}_1 - \mathbf{x}_2)/\varrho$ hence, $\mathbf{x}_2 = \mathbf{x}_1 - \nu\varrho$. Using $B_\varrho = \varrho S$ and changing variables $\nu \mapsto -\nu$, we obtain

$$(67) \quad -\varrho^{n-1} \int_S \int_S \nu \cdot (\theta_1 - \theta_2) \tilde{\sigma}(\mathbf{x}_1, \mathbf{x}_1 + \nu\varrho, t, \theta_1, \theta_2) d\theta_2 d\nu .$$

We split the outer integral into $S = S_+ \cup S_- = \{\nu \cdot (\theta_1 - \theta_2) > 0\} \cup \{\nu \cdot (\theta_1 - \theta_2) < 0\}$, where the two individuals move towards, resp. away from, each other, hence

$$\begin{aligned} & -\varrho^{n-1} \int_S \int_S \nu \cdot (\theta_1 - \theta_2) \tilde{\sigma}(\mathbf{x}_1, \mathbf{x}_1 + \nu\varrho, t, \theta_1, \theta_2) d\theta_2 d\nu \\ &= -\varrho^{n-1} (N-1) \left[\int_{S_+} \int_S \nu \cdot (\theta_1 - \theta_2) \tilde{\sigma}(\mathbf{x}_1, \mathbf{x}_1 + \nu\varrho, t, \theta_1, \theta_2) d\theta_2 d\nu \right. \\ & \quad \left. + \int_{S_-} \int_S \nu \cdot (\theta_1 - \theta_2) \tilde{\sigma}(\mathbf{x}_1, \mathbf{x}_1 + \nu\varrho, t, \theta_1, \theta_2) d\theta_2 d\nu \right] . \end{aligned}$$

In S_- we use the collision transformation defined in [Section 3](#), with new directions θ'_1, θ'_2 after collision, and normal vector $-\nu$:

$$\begin{aligned} & -\varrho^{n-1} \int_S \int_S \nu \cdot (\theta_1 - \theta_2) \tilde{\sigma}(\mathbf{x}_1, \mathbf{x}_1 + \nu\varrho, t, \theta_1, \theta_2) d\theta_2 d\nu \\ &= \varrho^{n-1} (N-1) \int_{S_+} \int_S \nu \cdot (\theta_1 - \theta_2) \left[\tilde{\sigma}(\mathbf{x}_1, \mathbf{x}_1 - \nu\varrho, t, \theta'_1, \theta'_2) \right. \\ & \quad \left. - \tilde{\sigma}(\mathbf{x}_1, \mathbf{x}_1 + \nu\varrho, t, \theta_1, \theta_2) \right] d\theta_2 d\nu . \end{aligned}$$

Appendix B. Study of alignment conditions. In this appendix we consider a specific form of the interaction kernel K^ε and different strengths of the alignment ℓ . We study the effect of these changes on the final system [\(48\)](#)-[\(49\)](#).

Let the influence kernel $K^\varepsilon \left(\frac{|\mathbf{y}-\mathbf{x}|}{\varepsilon} \right) = B^{-n} e^{-\frac{|\mathbf{y}-\mathbf{x}|}{\varepsilon B}}$, where B is a constant. In the case of short range alignment, $B \ll 1$, the flux term [\(42\)](#) can be rewritten as

$$(68) \quad \mathcal{J}(\mathbf{x}, t) = B^{-n} \int e^{-\frac{|\mathbf{y}-\mathbf{x}|}{\varepsilon B}} w(\mathbf{y}, t) d\mathbf{y} = \varepsilon^n \int e^{-|\mathbf{y}|} w(B\varepsilon\mathbf{y} + \mathbf{x}, t) d\mathbf{y} .$$

Taylor expansion of $w(B\varepsilon\mathbf{y} + \mathbf{x}, t)$ around $B = 0$ leads to (with constants D_1, D_2)

$$\mathcal{J}(\mathbf{x}, t) = D_1 \varepsilon^n w(\mathbf{x}, t) + D_2 \varepsilon^{n+2} B^2 \Delta w(\mathbf{x}, t) + \mathcal{O}(\varepsilon^{n+4} B^4) .$$

For the alignment vector Λ^w , we therefore find

$$(69) \quad \Lambda^w = \frac{\mathcal{J}(\mathbf{x}, t)}{|\mathcal{J}(\mathbf{x}, t)|} = \frac{w}{|w|} + \varepsilon^2 B^2 \frac{D_2}{D_1} \frac{|w|^2 \Delta w - w(w \cdot \Delta w)}{|w|^3} + \mathcal{O}(\varepsilon^4 B^4) .$$

Substituting into [\(49\)](#) we obtain the mean direction w

$$w \left(1 - \ell \frac{G(u)}{|w|F(u)} + \mathcal{O}(\varepsilon^2 B^2) \right) = -\frac{1}{F(u)} C_\alpha \nabla^{\alpha-1} u .$$

In this way we write w as an explicit function of u in the system (48)-(49).

On the other hand, if the alignment is weak in (49) i.e., $\ell \ll 1$, we note

$$(70) \quad w = -\frac{1}{F(u)}C_\alpha \nabla^{\alpha-1}u + \ell \frac{G(u)}{F(u)}\Lambda^u + \mathcal{O}(\ell^2),$$

where Λ^u is written in terms of

$$\mathcal{J}^u(\mathbf{x}, t) = -C_\alpha \int K^\varepsilon \left(\frac{|\mathbf{y} - \mathbf{x}|}{\varepsilon} \right) \frac{\nabla^{\alpha-1}u(\mathbf{y}, t)}{F(u(\mathbf{y}, t))} d\mathbf{y}.$$

In this case, the mean direction of motion of the individuals is dominated by the long runs described by the first term in (70), the alignment condition is of lower order.

Appendix C. Chapman-Enskog expansion. To formally derive the expansion (54), we start from (51) and substitute (52),

$$(71) \quad \begin{aligned} \varepsilon(\lambda + c_0\theta \cdot \nabla)\hat{p} - \varepsilon p_0 &= |S|(1 - \zeta)\Phi(\Lambda \cdot \theta) \left[\varepsilon^{-\mu}A + \varepsilon^{\mu(\alpha-2)+\alpha-1}B\lambda^{\alpha-1} \right] T_0\hat{p} \\ &- (\mathbb{1} - \zeta T) \left[\varepsilon^{-\mu}A + \varepsilon^{\mu(\alpha-2)+\alpha-1}B(\lambda + c_0\theta \cdot \nabla)^{\alpha-1} \right] \hat{p} + \mathcal{O}(\varepsilon), \end{aligned}$$

where we have defined $T_0\hat{p} = |S|^{-1} \int_S \hat{p} d\theta$.

To the leading order $\varepsilon^{-\mu}$, Equation (71) says

$$(72) \quad 0 = |S|(1 - \zeta)\Phi(\Lambda \cdot \theta) \frac{\alpha - 1}{\varsigma_0} T_0\hat{p}_0 - (\mathbb{1} - \zeta T) \frac{\alpha - 1}{\varsigma_0} \hat{p}_0,$$

or equivalently $\hat{p}_0 = \left[|S|(1 - \zeta)\Phi(\Lambda \cdot \theta)T_0 + \zeta T \right] \hat{p}_0$. For arbitrary $\zeta \in [0, 1]$ and, for simplicity, $T = T_0$ in (71), the leading order of the solution \hat{p}_0 is given by

$$(73) \quad \hat{p}_0(\mathbf{x}, t, \theta) = \Phi_\zeta(\theta)\hat{u}(\mathbf{x}, t),$$

with $\Phi_\zeta(\theta) = |S|(1 - \zeta)\Phi(\Lambda \cdot \theta) + \zeta$. When only alignment is considered, $\zeta = 0$, this reduces to the Chapman-Enskog expansion $\hat{p}_0 = \Phi(\Lambda \cdot \theta)\hat{u}$ obtained in [14, 21], while for run and tumble processes, $\zeta = 1$, one recovers the leading term of the eigenfunction expansion $\hat{p}_0 = T\hat{p}_0 = |S|^{-1}(\hat{u} + n\theta \cdot \hat{w})$ [15].

The next order of the expansion $\hat{p} = \hat{p}_0 + \varepsilon^m\hat{p}_1 + \mathcal{O}(\varepsilon^{2(\mu+1)(\alpha-1)})$, with $m = (\mu + 1)(\alpha - 1)$, is obtained from terms of order $\varepsilon^{\mu(\alpha-2)+\alpha-1}$ in (71):

$$(74) \quad (\mathbb{1} - \Phi_\zeta(\theta)T_0)\hat{p}_1 = \frac{1}{A} \left[(1 - \zeta)\Phi(\Lambda \cdot \theta)B\lambda^{\alpha-1} - (\mathbb{1} - \zeta T_0)B(\lambda + c_0\theta \cdot \nabla)^{\alpha-1}\Phi_\zeta(\theta) \right] \hat{u}.$$

where A and B are given in (53).

REFERENCES

- [1] M. AINSWORTH AND C. GLUSA, *Aspects of an adaptive finite element method for the fractional Laplacian: a priori and a posteriori error estimates, efficient implementation and multigrid solver*, Computer Methods in Applied Mechanics and Engineering, 327 (2017), pp. 4–35.
- [2] W. ALT, *Biased random walk models for chemotaxis and related diffusion approximations*, Journal of Mathematical Biology, 9 (1980), pp. 147–177.

- [3] B. G. ANDERSON, E. LOESER, M. GEE, F. REN, S. BISWAS, O. TURANOVA, M. HABERLAND, AND A. L. BERTOZZI, *Quantitative assessment of robotic swarm coverage*, arXiv preprint arXiv:1806.02488, (2018).
- [4] N. BELLOMO AND J. SOLER, *On the mathematical theory of the dynamics of swarms viewed as complex systems*, *Mathematical Models and Methods in Applied Sciences*, 22 (2012), p. 1140006.
- [5] M. BOSTAN AND J. A. CARRILLO, *Reduced fluid models for self-propelled particles interacting through alignment*, *Mathematical Models and Methods in Applied Sciences*, 27 (2017), pp. 1255–1299.
- [6] M. BRAMBILLA, E. FERRANTE, M. BIRATTARI, AND M. DORIGO, *Swarm robotics: a review from the swarm engineering perspective*, *Swarm Intelligence*, 7 (2013), pp. 1–41.
- [7] C. CERCIGNANI, R. ILLNER, AND M. PULVIRENTI, *The mathematical theory of dilute gases*, vol. 106, Springer Science & Business Media, 2013.
- [8] M. S. COUCEIRO, P. A. VARGAS, R. P. ROCHA, AND N. M. FERREIRA, *Benchmark of swarm robotics distributed techniques in a search task*, *Robotics and Autonomous Systems*, 62 (2014), pp. 200–213.
- [9] M. DE JAGER, F. J. WEISSING, P. M. HERMAN, B. A. NOLET, AND J. VAN DE KOPPEL, *Lévy walks evolve through interaction between movement and environmental complexity*, *Science*, 332 (2011), pp. 1551–1553.
- [10] P. DEGOND, *Macroscopic limits of the Boltzmann equation: a review*, in *Modeling and Computational Methods for Kinetic Equations*, Springer, 2004, pp. 3–57.
- [11] P. DEGOND, A. FROUVELLE, AND J.-G. LIU, *Macroscopic limits and phase transition in a system of self-propelled particles*, *Journal of Nonlinear Science*, 23 (2013), pp. 427–456.
- [12] P. DEGOND AND S. MOTSCH, *Continuum limit of self-driven particles with orientation interaction*, *Mathematical Models and Methods in Applied Sciences*, 18 (2008), pp. 1193–1215.
- [13] A. DHARIWAL, G. S. SUKHATME, AND A. A. REQUICHA, *Bacterium-inspired robots for environmental monitoring*, in *Robotics and Automation, 2004. Proceedings. ICRA'04. 2004 IEEE International Conference on*, vol. 2, IEEE, 2004, pp. 1436–1443.
- [14] G. DIMARCO AND S. MOTSCH, *Self-alignment driven by jump processes: Macroscopic limit and numerical investigation*, *Mathematical Models and Methods in Applied Sciences*, 26 (2016), pp. 1385–1410.
- [15] G. ESTRADA-RODRIGUEZ, H. GIMPERLEIN, AND K. J. PAINTER, *Fractional Patlak–Keller–Segel equations for chemotactic superdiffusion*, *SIAM Journal on Applied Mathematics*, 78 (2018), pp. 1155–1173.
- [16] G. ESTRADA-RODRIGUEZ, H. GIMPERLEIN, K. J. PAINTER, AND J. STOCEK, *Space-time fractional diffusion in cell movement models with delay*, arXiv preprint arXiv:1802.08675, (2018).
- [17] B. FRANZ, J. P. TAYLOR-KING, C. YATES, AND R. ERBAN, *Hard-sphere interactions in velocity-jump models*, *Physical Review E*, 94 (2016), p. 012129.
- [18] G. M. FRICKE, J. P. HECKER, J. L. CANNON, AND M. E. MOSES, *Immune-inspired search strategies for robot swarms*, *Robotica*, 34 (2016), pp. 1791–1810.
- [19] S.-Y. HA AND E. TADMOR, *From particle to kinetic and hydrodynamic descriptions of flocking*, *Kinetic & Related Models*, 1 (2008), pp. 415–435.
- [20] T. HARRIS ET AL., *Generalized Lévy walks and the role of chemokines in migration of effector CD8+ T cells*, *Nature*, 486 (2012), pp. 545–548.
- [21] B. JACEK ET AL., *Singularly perturbed evolution equations with applications to kinetic theory*, vol. 34, World Scientific, 1995.
- [22] A. JADBABAIE, J. LIN, AND A. S. MORSE, *Coordination of groups of mobile autonomous agents using nearest neighbor rules*, *IEEE Transactions on Automatic Control*, 48 (2003), pp. 988–1001.
- [23] G. KANTOR, S. SINGH, R. PETERSON, D. RUS, A. DAS, V. KUMAR, G. PEREIRA, AND J. SPLETZER, *Distributed search and rescue with robot and sensor teams*, in *Field and Service Robotics*, Springer, 2003, pp. 529–538.
- [24] E. H. KENNARD ET AL., *Kinetic theory of gases, with an introduction to statistical mechanics*, McGraw-Hill, 1938., 1938.
- [25] E. KOROBKOVA, T. EMONET, J. M. VILAR, T. S. SHIMIZU, AND P. CLUZEL, *From molecular noise to behavioural variability in a single bacterium*, *Nature*, 428 (2004), pp. 574–578.
- [26] M. KRIVONOSOV, S. DENISOV, AND V. ZABURDAEV, *Lévy robotics*, arXiv preprint arXiv:1612.03997, (2016).
- [27] X. LI, *Adaptively choosing neighbourhood bests using species in a particle swarm optimizer for multimodal function optimization*, in *Genetic and Evolutionary Computation Conference*, Springer, 2004, pp. 105–116.

- [28] F. MONDADA AND ET AL., *The e-puck, a robot designed for education in engineering*, in Proceedings of the 9th Conference on Autonomous Robot Systems and Competitions, 2009, pp. 59–65.
- [29] S. MOTSCH AND E. TADMOR, *A new model for self-organized dynamics and its flocking behavior*, Journal of Statistical Physics, 144 (2011), p. 923.
- [30] S. G. NURZAMAN, Y. MATSUMOTO, Y. NAKAMURA, S. KOIZUMI, AND H. ISHIGURO, *Yuragi-based adaptive searching behavior in mobile robot: From bacterial chemotaxis to Lévy walk*, in Robotics and Biomimetics, 2008. ROBIO 2008. IEEE International Conference on, IEEE, 2009, pp. 806–811.
- [31] H. G. OTHMER AND T. HILLEN, *The diffusion limit of transport equations derived from velocity-jump processes*, SIAM Journal on Applied Mathematics, 61 (2000), pp. 751–775.
- [32] Z. PASTERNAK, F. BARTUMEUS, AND F. W. GRASSO, *Lévy-taxis: a novel search strategy for finding odor plumes in turbulent flow-dominated environments*, Journal of Physics A: Mathematical and Theoretical, 42 (2009), p. 434010.
- [33] C. S. PATLAK, *Random walk with persistence and external bias*, The Bulletin of Mathematical Biophysics, 15 (1953), pp. 311–338.
- [34] B. PERTHAME, W. SUN, AND M. TANG, *The fractional diffusion limit of a kinetic model with biochemical pathway*, Zeitschrift für angewandte Mathematik und Physik, 69 (2018), p. 67.
- [35] G. RAMOS-FERNÁNDEZ, J. L. MATEOS, O. MIRAMONTES, G. COCHO, H. LARRALDE, AND B. AYALA-OROZCO, *Lévy walk patterns in the foraging movements of spider monkeys (Atles geoffroyi)*, Behavioral Ecology and Sociobiology, 55 (2004), pp. 223–230.
- [36] A. SCHROEDER, S. RAMAKRISHNAN, M. KUMAR, AND B. TREASE, *Efficient spatial coverage by a robot swarm based on an ant foraging model and the Lévy distribution*, Swarm Intelligence, 11 (2017), pp. 39–69.
- [37] M. SENANAYAKE, I. SENTHOORAN, J. C. BARCA, H. CHUNG, J. KAMRUZZAMAN, AND M. MURSHED, *Search and tracking algorithms for swarms of robots: A survey*, Robotics and Autonomous Systems, 75 (2016), pp. 422–434.
- [38] J. SHEN, *Cucker–Smale flocking under hierarchical leadership*, SIAM Journal on Applied Mathematics, 68 (2007), pp. 694–719.
- [39] R. SHVYDKOY AND E. TADMOR, *Topological models for emergent dynamics with short-range interactions*, arXiv preprint arXiv:1806.01371, (2018).
- [40] D. K. SUTANTYO, S. KERNBACH, P. LEVI, AND V. A. NEPOMNYASHCHIKH, *Multi-robot searching algorithm using Lévy flight and artificial potential field*, in Safety Security and Rescue Robotics (SSRR), 2010 IEEE International Workshop on, IEEE, 2010, pp. 1–6.
- [41] Y. TAN AND Z.-Y. ZHENG, *Research advance in swarm robotics*, Defence Technology, 9 (2013), pp. 18–39.
- [42] J. P. TAYLOR-KING, B. FRANZ, C. A. YATES, AND R. ERBAN, *Mathematical modelling of turning delays in swarm robotics*, IMA Journal of Applied Mathematics, 80 (2015), pp. 1454–1474.
- [43] J. P. TAYLOR-KING, R. KLAGES, S. FEDOTOV, AND R. A. VAN GORDER, *Fractional diffusion equation for an n-dimensional correlated Lévy walk*, Physical Review E, 94 (2016), p. 012104.
- [44] M. TURDUEV, M. KIRTAY, P. SOUSA, V. GAZI, AND L. MARQUES, *Chemical concentration map building through bacterial foraging optimization based search algorithm by mobile robots*, in Systems Man and Cybernetics (SMC), 2010 IEEE International Conference on, IEEE, 2010, pp. 3242–3249.
- [45] G. VARELA, P. CAAMAÑO, F. ORJALES, Á. DEIBE, F. LOPEZ-PENA, AND R. J. DURO, *Swarm intelligence based approach for real time uav team coordination in search operations*, in Nature and Biologically Inspired Computing (NaBIC), 2011 Third World Congress on, IEEE, 2011, pp. 365–370.
- [46] T. VICSEK, A. CZIRÓK, E. BEN-JACOB, I. COHEN, AND O. SHOCHET, *Novel type of phase transition in a system of self-driven particles*, Physical review letters, 75 (1995), p. 1226.
- [47] C. XUE, H. G. OTHMER, AND R. ERBAN, *From individual to collective behavior of unicellular organisms: recent results and open problems*, in AIP Conference Proceedings, vol. 1167, AIP, 2009, pp. 3–14.